IEEE Access
Multidisciplinary | Rapid Review | Open Access Journal

Received September 29, 2021, accepted November 5, 2021, date of publication November 15, 2021,
date of current version November 23, 2021.

Digital Object Identifier 10.1109/ACCESS.2021.3128154

A 20-80 MHz Continuously Tunable Gm-C Low-Pass Filter for Ultra-Low Power WBAN Receiver Front-End

XIAOYING WANG, (Student Member, IEEE), CHIRN CHYE BOON, (Senior Member, IEEE), KAITUO YANG, (Member, IEEE), AND LINGSHAN KONG
CICS Laboratory, School of Electrical and Electronic Engineering, Nanyang Technological University, Singapore 639798

Corresponding author: Chirn Chye Boon (eccboon@ntu.edu.sg)

This work was supported by the Singapore Ministry of Education Academic Research Fund Tier 2 under Grant MOE2019-T2-1-114.

ABSTRACT This paper presents a third-order Butterworth low-pass filter (LPF) with continuously tuning capability to be used in the receiver front-end for Wireless Body Area Network (WBAN). To realize the bandwidth tuning for multi-standard operation in WBAN receivers with ultra-low power consumption and minimized area, a novel transconductor-capacitor (Gm-C) filter is proposed. The proposed transconductor core uses an additional gain stage with regulated cascode structure to control the transconductance (G_m) by tuning the drain-source voltage V_{ds} of the input transistors operating in linear region. Based on fundamental analysis, V_{ds} should be reduced to attenuate the nonlinear effects caused by higher-order harmonic components. This proposed transconductor circuit enables the G_m tuning and widens the tuning range while maintaining good linearity with negligible power and area consumption. This work is then implemented into a third-order Butterworth LPF. Measurements show that with external control voltage varying from 450 mV to 550 mV, the cutoff frequency of the LPF can be continuously adjusted from 20 MHz to 80 MHz. This design is implemented in 40 nm CMOS process with 1.1 V supply voltage. The total power consumption of this work is below 2 mW with an active area of 0.0105 mm^2. Its low power consumption and good area efficiency makes this LPF suitable for WBAN applications.

INDEX TERMS CMOS low-pass filter (LPF), Gm-C, ultra-low power, Butterworth filter, wireless body area network (WBAN).

I. INTRODUCTION

The rapid development in biomedical devices shows the rising public concern towards health topic. Moreover, the advancement in wireless technologies and radio frequency communications enables the evolution of ''e-health'' services, allowing healthcare providers to efficiently administer and deliver a great variety of healthcare services. Health information including vital signs and emotion statuses can be closely monitored at anytime, anywhere. Doctors may be alerted in case of emergencies [1].

One key technology that aligns with ''e-health'' concept, namely, wireless body area network (WBAN), describes the wireless network that builds the communication channel between tiny physiological signal sensors and central controlling unit for monitoring purpose [1]. Notably, for medical data transmission, it is crucial to carefully select and adjust the operating frequency bands to avoid loss of accuracy and reduce the latency of wireless data transfer. In-time transmission of data is always critical in medical data monitoring especially when alerting emergencies. Besides, power and area consumption are also important attributes for WBAN devices. Especially for those implanted WBAN devices, long battery life and miniature size can largely improve the quality of service (QoS). Supporting by IEEE 802.15.6 standard [2], a fully on-chip receiver front-end block shown in Fig. 1 undertakes the coordination task in between the central processing unit and the sensing front-end in the WBAN system. Receivers, as the entry block of the entire wireless transceiver systems, play a crucial role in quantifying system's performance and reliability [3]–[5]. In order to support multi-standard operation, passband reconfigurability of the filtering block in the

The associate editor coordinating the review of this manuscript and approving it for publication was Emrecan Demirors.

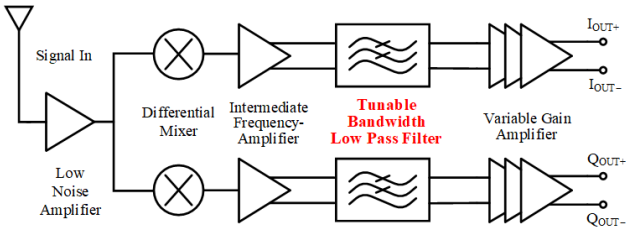

FIGURE 1. Fully on-chip receiver front-end block diagram.

WBAN receivers becomes necessary. Besides, the filter shall not add extra power and area expense to the entire receiver. This paper provides a low-pass reconfigurable filtering solution at high frequency while meeting the stringent power and area requirements for short-range WBAN communications.

Over the years, various low-voltage active filter designs have been well developed. Among these, active resistor-capacitor (active-RC) topology and transconductor-C (Gm-C) topology are popular choices in wireless communication applications. As illustrated in Fig. 2 (a), the active-RC topology shows good linearity performance, but the lack of local feedback around its active elements results in the limited filter's bandwidth [6]–[9]. Using resistive elements also results in high power and large area consumption, making such topology less attractive to today's WBAN market. On the contrary, as shown in Fig. 2 (b), the open-loop operation of the Gm-C topology suggests a reduction in power consumption as compared to the active-RC topology, even at high frequency. Moreover, previous works suggest that when the transconductance value G_m or the capacitance value C are tuned, we can control the frequency response of the Gm-C filter for multi-standard wireless receiver systems [11], [15], [16]. The digitally configurable OTA in [16] allows continuous tuning of G_m whereas the other capacitive tuning method in [15] adopts the programmable capacitor bank with control logic to digitally tune C. In fact, the digitally tuned OTAs in the former Gm-C topology employ power-hungry common-mode feedback circuitry and also show poor linearity. The large area occupied by the capacitor bank brings up the area concern for WBAN devices.

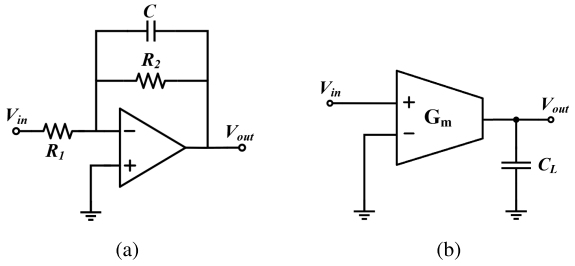

FIGURE 2. (a) An active-RC integrator; (b) a Gm-C integrator.

For short-range WBAN devices or corresponding peripherals, power consumption, linearity performance and area efficiency are all important attributes. Therefore, this work addresses these issues where we propose a novel G_m-tunable transconductor topology. The proposed circuit achieves tuning capability with improved linearity through the novel regulated cascode structure. The use of an additional gain stage with a cascode transistor regulates the drain-source voltage of the input transistor and also forms a feedback loop to boost the output impedance. In addition, a level shifter is added in between the gain stage and the input transistor to achieve wide tuning range and further improve the linearity. By using the single-stage amplifier as the gain stage and making the input transistors operating in linear region, ultra-low power is achieved in this work. Furthermore, the third-order Butterworth filter realized by the proposed transconductor occupies small chip area since the G_m tuning scheme with fixed capacitors largely reduces the area as compared to those conventional designs with the capacitor bank.

This paper is structured into four sections. Firstly, section I serves as the introduction. Section II begins with the Butterworth filter design and continues with the proposed fully differential transconductor core with novel tuning structure. With the common-mode feedback, the complete fully differential third-order low-pass filter is shown with the proposed transconductor cells. Measurement results and comparison table are presented in Section III and conclusions are drawn in the last section.

II. PROPOSED THIRD-ORDER LPF WITH TUNING CAPABILITY

In this section, the Butterworth structure is first introduced to explain the filter's operation. Then the proposed tunable regulated cascode transconductor core is analyzed in detail. Lastly, the complete design is presented with common-mode feedback.

A. THIRD-ORDER BUTTERWORTH LOW-PASS FILTER

For a low-pass analog filter, the generalized transfer function is given as

$$T(s) = \frac{N(s)}{D(s)} = K\frac{(s-z_1)(s-z_2)\cdots(s-z_m)}{(s-p_1)(s-p_2)\cdots(s-p_n)} \quad (1)$$

where the coefficients m, n and K are real numbers and the imaginary part s introduces the frequency components. The z_i's are the roots to the equation $N(s) = 0$, representing that when $s = z_i$ the transfer function "vanishes"; whereas the p_j's are the answers to the equation $D(s) = 0$, indicating the value of the transfer function becomes unbounded when $s = p_j$. Poles and zeros define the transfer characteristic of a filter. In Bode plot, pole frequencies correspond to the decreasing of magnitude response by 20 dB per decade. Contrarily, the slope of the magnitude curve will increase by the same ratio when coming across a zero frequency.

Not surprisingly, numerous approximation methods on the frequency response have been raised such as elliptic, Chebyshev, Butterworth, and many others. Out of those classic methods, Butterworth filter is chosen due to its "maximally flat" response and hence most suitable in this low-pass filter

design for the WBAN system [10], [11]. Higher-order Butterworth filters are constructed by cascading lower-order ones. Here, the proposed third-order low-pass filter begins with a lossy integrator as the first-order block and is cascaded by a biquadratic cell as the second-order block. The generalized transfer function is given as

$$T(s) = \frac{N(s)}{D(s)} = K\frac{1}{(s-p_1)(s-p_2)(s-p_3)} = K'\frac{1}{(s-p_1)}\cdot\frac{\omega_0^2}{s^2+(\omega_0/Q)s+\omega_0^2} \quad (2)$$

The first pole is created by the first-order Gm-C filter shown in Fig. 3 (a). The Kirchhoff's current law is applied on node X to obtain its first-order response as in (3). The fraction a in this design is set to zero so that the result follows a low-pass frequency response and create a pole in the final transfer function.

$$T_1(s) = \frac{a\cdot sC_0 + G_{m1}}{sC_0 + G_{m2}} = \frac{G_m/C_0}{s+G_m/C_0} \quad (3)$$

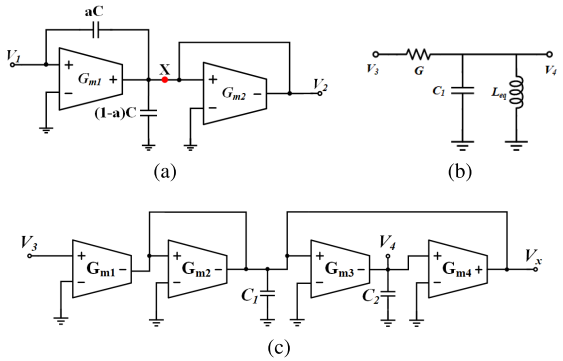

FIGURE 3. (a) First-order stage: a single-ended Gm-C lossy integrator; (b) RLC prototype for Biquadratic cell; (c) second-order stage: a single-ended Biquadratic cell.

The biquadratic cell, derived from the RLC ladder network prototype in Fig. 3 (b), contributes two poles to the final frequency response. As shown in Fig. 3 (c), G_{m1} performs voltage to current conversion but with a reversed polarity to obtain a positive output V_4 integrated from V_x. G_{m2} replaces the resistor G while the capacitor C_1 stays unchanged. The subsequent gyrator cell formed by G_{m3} and G_{m4} together with another capacitor C_2 has an equivalent inductance as in (5).

$$T_2(s) = \frac{V_4}{V_3} = \frac{\frac{G_m^2}{C_1C_2}}{s^2+\left(\frac{G_m}{C_1}\right)s+\left(\frac{G_m^2}{C_1C_2}\right)} \quad (4)$$

$$L_{eq} = \frac{C_2}{G_{m3}G_{m4}} \quad (5)$$

To improve the system's stability, the final circuit is converted into fully differential structure. By integrating the transfer functions of the two stages, the final frequency response can then be derived with the device parameters.

$$T(s) = \frac{V_{out}}{V_{in}} = \frac{\left(\frac{G_m}{C_0}\right)}{s+\left(\frac{G_m}{C_0}\right)}\cdot\frac{\left(\frac{G_m^2}{C_1C_2}\right)}{\left[s^2+\left(\frac{G_m}{C_0}\right)s+\left(\frac{G_m^2}{C_1C_2}\right)\right]}$$

$$\omega_0 = \sqrt{\frac{G_m^2}{C_1C_2}}, \quad \frac{\omega_0}{Q} = \frac{G_m}{C_1} \Longrightarrow Q = \sqrt{\frac{C_1}{C_2}}$$

In this work, identical transconductor cells are employed, implying the same G_m values throughout the entire LPF block. In the lossy integrator stage, the dc gain is unity and the capacitance C_0 is chosen such that $\omega_0 C_0 \ll G_m$, resulting in a negligible effect from C_0 over the bandwidth of interest. Then the biquadratic section contributes to the -3 dB attenuation at the passband corner, where we need $|T_2(s)|_{s^2=-\omega_0^2} = Q$. The quality factor Q is $\sqrt{1/2}$ so we have $2C_1 = C_2$. In such way, the third-order low-pass filtering can be realized. Through the tuning of either G_m or the capacitance value, the filter's cutoff frequency is determined. With such tunable frequency response, we can obtain the prototype of the bandwidth-tunable third-order Butterworth LPF, where we propose a novel transconductor circuit to meet the WBAN network design requirements.

B. PROPOSED ULTRA-LOW POWER TUNABLE TRANSCONDUCTOR WITH ENHANCED LINEARITY

Tuning capability is crucial for the LPF in multi-standards WBAN applications. In the Gm-C filters, the cutoff frequency is proportional to the G_m value and inversely proportional to the capacitance C. Literature mainly chose to tune the bandwidth with programmable capacitor arrays to prevent linearity distortion [14]–[16]. However, the capacitor array occupies large chip area and consumes extra power, which is less favorable to meet WBAN standards. In this work, the tuning scheme is fulfilled by tuning the G_m values in the identical transconductor cells in the third-order Butterworth LPF.

In the transconductor cell, the conversion from the input voltages to the output currents is quantified by the linear transconductance factor G_m. As illustrated in Fig. 4, the current flowing through the common-source transistors M1

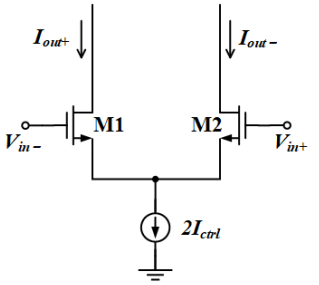

FIGURE 4. A simple transconductor core.

and M2 controls their transconductance values. The operation regions of the transistors are usually the identifier for classifying various transconductors designs.

$$I_{o\_saturation} = \sqrt{2\beta I_{ctrl}} \cdot V_i \cdot \sqrt{1 - \frac{\beta \cdot V_i^2}{4(V_{gs} - V_{th})}} \quad (6)$$

$$I_{o\_triode} = \beta V_{ds}(V_{gs1} - V_{gs2}) \quad (7)$$

where $V_i = V_{gs1} - V_{gs2}$ and β is the coefficient defined by the physical properties of the transistor. On such account, (6) shows that the transconductance I_o/V_i is linear only when V_{gs} is large enough and reaches velocity saturation, which contrasts with the prerequisite of low power design. However, we can easily observe a linear relationship between input voltage and output current in (7). This value, corresponding to a constant V_{ds} over the variation of V_{gs} and I_{ds}, defines the linear transconductance and is represented by G_m (or g_m in small-signal model).

$$G_m = g_m = \frac{\partial I_{ds}}{\partial V_{gs}} = \beta \cdot V_{ds} \quad (8)$$

As mentioned, the cutoff frequency in this work is tuned by varying individual G_m in each transconductor simultaneously. Equation (8) indicates that G_m can be controlled by the β factor or V_{ds}. However, the β factor is hard to change as it is related to the transistor's sizing and physical constraints. Hence, G_m value can only be tuned by controlling the drain-to-source voltage of the input transistors. As shown in Fig. 5 (a), the common-source transistor M2 functions as a negative feedback amplifier to fix V_{ds1} at a constant level so that the input transistor M1 operates in the triode region. The corresponding transfer characteristic should consider various factors including the second-order effects such as mobility degradation and parasitic capacitance. The Taylor expansion of the transistor model is applied to describe its *I-V* characteristic [12].

$$I_{out} = a_0 + a_1 V_{ds1} + a_2 (V_{ds1})^2 + a_3 (V_{ds1})^3 + \ldots \quad (9)$$

where the coefficient of the fundamental V_{ds1} term is given by $a_1 \approx \beta(V_{gs1} - V_{th})$. As the even-order terms are cancelled out through adopting the fully differential structure, the third-order term V_{ds1}^3 becomes the main source of non-linearity. To improve the linearity, one effective method is to reduce the V_{ds1} level to minimize higher-order terms in (9). Hence, one major drawback of this simple structure is the bias of the input transistors is restricted by V_{gs2} which leads to its modest linearity. Besides, its limited tuning range is another shortcoming of this structure, where $V_{ds1\_min} = V_{th2}$.

In this work, we propose a novel regulated cascode structure to allow a wider range of V_{ds1} tuning while lowering its value to improve linearity, as illustrated in Fig. 5 (b). The gain stage is an operational transconductance amplifier (OTA) that forms a feedback loop to achieve sufficiently large gain and hence boosts the output impedance of the transconductor. The output impedance is approximated as:

$$R_{out} = r_{o1} + r_{o3} + A g_{m3} r_{o1} r_{o3} \approx A g_{m3} r_{o1} r_{o3} \quad (10)$$

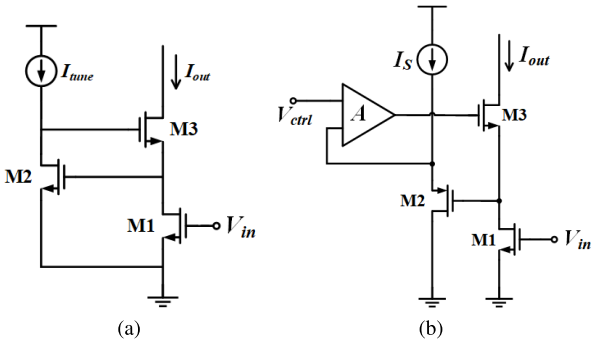

FIGURE 5. (a) A simple regulated cascode transconductor; (b) proposed wide-range regulated cascode transconductor.

The PMOS source follower M2 functioning as a level shifter is inserted to the inverting input of the OTA. This level shifter reduces the V_{ds1_min} of the input transistor M1 by an amount of V_{sg2} to widen the tuning range of the transconductor cell. As a result, we are able to tune the transconductance without degrading the linearity. Note that the body of M2 is connected to its own gate terminal with a floating well, so that voltage between its body and source V_{bs2} is zeroed, producing a constant threshold voltage V_{th2} for level shifting.

The amplifier together with the level shifter maintains V_{ds1} at a pre-determined level at $(V_{ctrl} - V_{sg2})$. In this way, the cascode amplifier "regulates" V_{ds1} and results in lesser variations in I_{out}. Meanwhile, this regulating structure maintains the triode operation region of the input transistor M1, with a simplified expression of its drain current $I_{D1} = \beta[(V_{gs1} - V_{th1})V_{ds1} - (V_{ds1}^2)/2]$. Finally, the transconductance becomes:

$$g_m \approx \frac{\beta_1 V_{ds1}}{1 + \dfrac{V_{gs3} - V_{th}}{A V_{ds1}}} = \frac{g_{m1}}{1 + \dfrac{2I_{D1}}{A g_{m3} V_{ds1}}} \quad (11)$$

Therefore, the gain offered by the amplifier increases the effective transconductance of M3 by A times and hence reduces the linearity error $2I_{D1}/(Ag_{m3}V_{ds1})$. The level shifter widens the tuning range with $V_{ds1\_min} = V_{ctrl} - V_{sg2}$, hence allowing the control of the voltage condition of M1 with better linearity. Continuous tuning of the passband is then possible by tuning V_{ctrl} whereas literature realized the tuning scheme by complex programming capacitor arrays [15]. Besides, simulations on dc operations also showed reduced power as compared with other G_m tuning designs [16]. Together with the simplified structure, this work realizes the tuning capability with good power and area efficiency.

In Fig. 6 (a), the proposed transconductor structure is transformed to fully differential structure to reduce the even-order non-linear elements caused by interference. In addition, to hold the output common mode level at constant, the common-mode feedback (CMFB) loop is implemented with dual-differential pair (DDP) common-mode detector topology based on current-steering principle, as depicted in Fig. 6 (b).

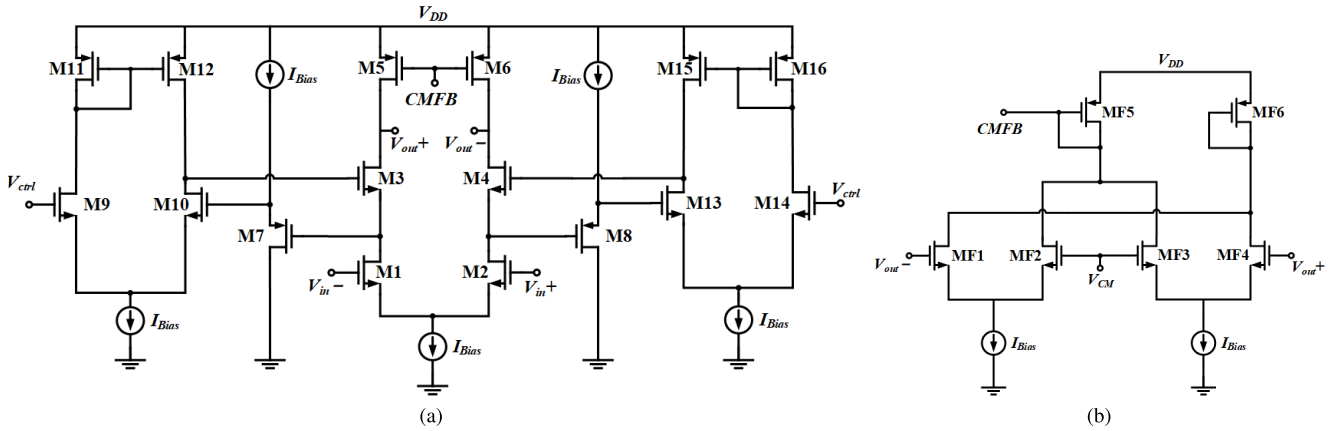

FIGURE 6. (a) Proposed fully differential transconductor core; (b) dual-differential Common Mode Feedback (CMFB) pair.

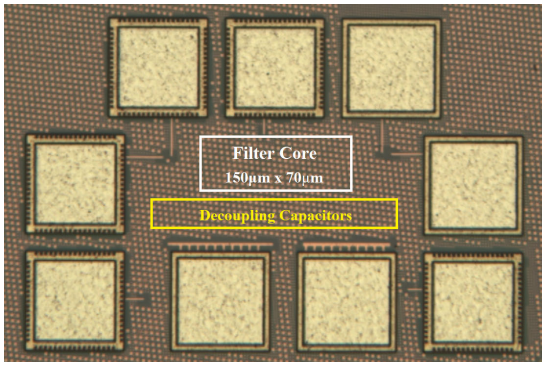

FIGURE 7. Die photo of the third-order low-pass filter.

III. MEASUREMENT RESULTS AND COMPARISON

The proposed third-order low-pass filter was designed and fabricated using TSMC 40 nm CMOS process. With input common-mode level at 550 mV (half of V_{DD}), the overall current consumption was 1.76 mA to 2.06 mA corresponding to the minimum and maximum V_{ctrl}. As shown in Fig. 7, this design occupies a core area of 0.0105 mm^2 (0.07 mm $\times$ 0.15 mm) and a total die area of 0.18 mm^2 (0.36 mm $\times$ 0.5 mm) including decoupling capacitors and I/O pads.

Post-layout simulations in Cadence® Virtuoso ADE and on-PCB measurements were performed subsequently to evaluate the performance. The test-bench for the LPF prototype was fed with 100 Ω differential input and 1.1 V supply. In the WBAN receiver front-end, the subsequent block following the filter is a variable gain amplifier (VGA) with extremely high input impedance. To preserve the consistency for the system design, the differential output in the test-bench is loaded with very high impedance, up to 100 kΩ.

First, the tunable frequency response was examined. V_{ctrl} represents the external control voltage that tunes the G_m value of the transconductor. Fig. 8 (a) and (b) shows the frequency response under different V_{ctrl} values for both post-layout simulation and on-PCB measurement. From the plot, we can

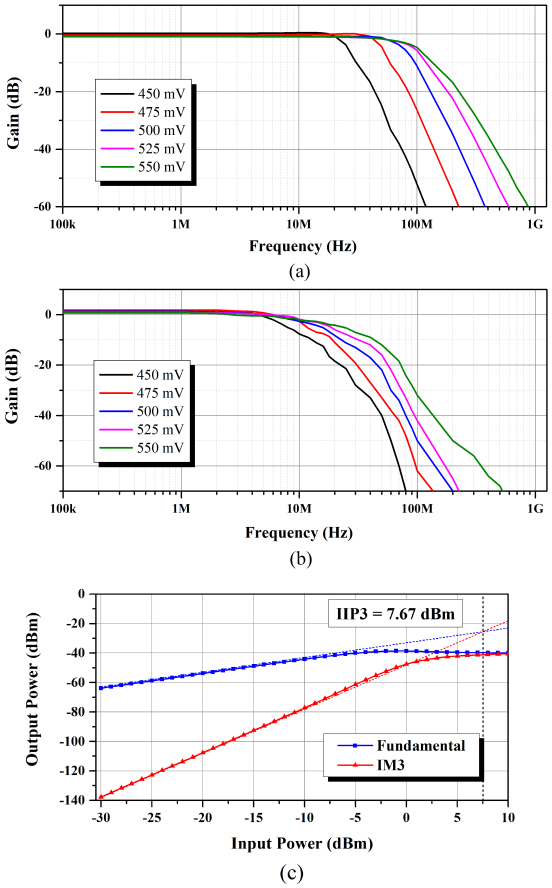

FIGURE 8. (a) Measured frequency response of the proposed filter; (b) post-layout simulated frequency response; (c) post-layout simulated input-referred IIP3 curve.

observe 20 MHz passband frequency change with every 25 mV voltage change, ranging from 450 mV to 550 mV and from 20 MHz to 80 MHz and it allows continuous and precise tuning within the tuning range. The anticipated impacts caused by additional capacitance from the off-chip

Balun and signal converters are the main reason of reduced cutoff frequencies in the measured results.

Other than the frequency response, the linearity of the filter was also evaluated. When the even-order harmonic terms are cancelled out in fully differential structure, the main source of nonlinearity is the third-order term. As shown in Fig. 8 (c), the input-referred third-order interception point (IIP3) is a hypothetical extrapolation point where the fundamental component intercepts with the third-order intermodulation products in the input-output power plot. The IIP3 value of this LPF is 7.67 dBm with 450 mV control voltage corresponding to the 20 MHz cutoff frequency.

In addition, a figure-of-merit (FoM) introduced in [13] is used to compare with relevant works.

$$FoM = \frac{P_C/N}{f_C \cdot (SFDR \cdot N^{4/3})} \tag{12}$$

$$SFDR = \left(\frac{IIP3}{P_N}\right)^{2/3} \tag{13}$$

where N is the number of poles and zeros, P_C/N is the normalized power consumption, and $SFDR \cdot N^{4/3}$ is the normalized spurious free dynamic range. With P_N denotes the input-referred noise power, the spurious-free dynamic range (SFDR) measured in *dBc* defines the dynamic ratio between the power of the fundamental signal and that of the next most significant spurious signal in frequency domain, hence accounting for both the filter's linearity and noise performance.

The important parameters are summarized in Table. 1 with literature. The active-RC design in [14] shows good linearity but the power consumption is rather high with lower tunable bandwidth. In [15], although the Gm-C filter adopts the current-reuse amplifiers to achieve lower FoM, the filter's cutoff frequency has no tuning capability and its higher-order frequency response increases the power consumption and the chip area. In addition, the work in [16] uses similar G_m tuning scheme, indicating that its nonlinear distortion is also caused by the triode-region input transistors. The FoM comparison suggests that this work achieves improved noise and linearity performance. To summarize, the proposed filter tunes the cutoff frequency continuously with wide tuning range. It also shows excellent power and area efficiency while maintaining comparable linearity. These features highlight the significance of this design in the WBAN receiver front-end implementation.

TABLE 1. Filter performance comparison with literature.

	This work	[14]	[15]	[16]
Technology	40 nm	65 nm	180 nm	180 nm
Supply (V)	1.1	1.8	1.8	1.8
Filter order	3	4	6	4
Transconductor topology	Gm-C	Active-RC	Gm-C	Gm-C
Bandwidth (MHz)	20-80	0.02-16	65	2.5-10.3
IIP3 (dBm)	7.67	22.1	12	-2.59-4.14
Power consumption (mW)	1.94-2.27	19	8.1	10.26-12.96
Core area (mm^2)	0.0105	0.098	0.21	0.23
FoM (fJ)	0.116	0.90	0.091	7.30-0.774

IV. CONCLUSION

In this paper, we have proposed an ultra-low power tunable third-order Butterworth Gm-C low-pass filter for multi-standard receivers for WBAN applications. By employing a novel regulated cascode OTA gain stage, the fully differential transconductor core allows continuous passband tuning from 20 MHz to 80 MHz while maintaining an IIP3 of 7.67 dBm. Fabricated in CMOS 40 nm process with 1.1 V supply voltage, measurements show that this design consumes 2 mW of power and occupies 0.0105 mm^2 of chip area. The low FoM of this work also shows its advantages in power consumption and noise performance. In conclusion, this design fulfills the filtering needs in advanced WBAN receivers.

REFERENCES

[1] R. Negra, I. Jemili, and A. Belghith, "Wireless body area networks: Applications and technologies," *Proc. Comput. Sci.*, vol. 83, pp. 1274–1281, Jan. 2016.

[2] *IEEE 802.15.6: Wireless Body Area Networks*, IEEE Standard 802.15.6-2012, Feb. 2012, pp. 1–271.

[3] A. C. W. Wong, M. Dawkins, G. Devita, N. Kasparidis, A. Katsiamis, O. King, F. Lauria, J. Schiff, and A. J. Burdett, "A 1 V 5 mA multimode IEEE 802.15. 6/Bluetooth low-energy WBAN transceiver for biotelemetry applications," *IEEE J. Solid-State Circuits*, vol. 48, no. 1, pp. 186–198, Jan. 2013.

[4] J. Cheng, N. Qi, P. Y. Chiang, and A. Natarajan, "A low-power, low-voltage WBAN-compatible sub-sampling PSK receiver in 65 nm CMOS," *IEEE J. Solid-State Circuits*, vol. 49, no. 12, pp. 3018–3030, Dec. 2014.

[5] J. O. Ha, S. H. Jung, M. C. Park, K. H. Lee, and Y. S. Eo, "A fully integrated 3–5 GHz UWB RF transceiver for WBAN applications," in *IEEE MTT-S Int. Microw. Symp. Dig.*, Dec. 2013, pp. 1–3.

[6] M. De Matteis, S. D'Amico, and A. Baschirotto, "A 0.55 V 60 dB-DR fourth-order analog baseband filter," *IEEE J. Solid-State Circuits*, vol. 44, no. 9, pp. 2525–2534, Sep. 2009.

[7] P. Khumsat and A. Worapishet, "A 0.5-v r-MOSFET-C filter design using subthreshold R-MOSFET resistors and OTAs with cross-forward common-mode cancellation technique," *IEEE J. Solid-State Circuits*, vol. 47, no. 11, pp. 2751–2762, Nov. 2012.

[8] F. Lavalle-Aviles and E. Sánchez-Sinencio, "A 0.6-V power-efficient active-RC analog low-pass filter with cutoff frequency selection," *IEEE Trans. Very Large Scale Integr. (VLSI) Syst.*, vol. 28, no. 8, pp. 1757–1769, May 2020.

[9] L. Lei, C. Tao, Z. Hong, and Y. Huang, "A 5.7 mW +30 dBm IIP3, tunable active-RC LPF in 40 nm CMOS," in *Proc. IEEE Int. Symp. Circuits Syst. (ISCAS)*, May 2021, pp. 1–4.

[10] J. Perez-Bailon, A. Marquez, B. Calvo, and N. Medrano, "A 0.18 μm CMOS widely tunable low pass filter with sub-Hz cutoff frequencies," in *Proc. IEEE Int. Symp. Circuits Syst. (ISCAS)*, May 2018, pp. 1–4.

[11] C. Yehoshuva, R. Rakhi, D. Anto, and S. Kaurati, "0.5 V, ultra low power multi standard G_m-C filter for biomedical applications," in *Proc. IEEE Int. Conf. Recent Trends Electron., Inf. Commun. Technol. (RTEICT)*, May 2016, pp. 165–169.

[12] T. Ndjountche, *CMOS Analog Integrated Circuits: High-Speed and Power-Efficient Design*. Boca Raton, FL, USA: CRC Press, 2011.
[13] S. Hori, T. Maeda, h. Yano, N. Matsuno, K. Numata, N. Yoshida, Y. Takahashi, T. Yamase, R. Walkington, and H. Hikaru, "A widely tunable CMOS Gm-C filter with a negative source degeneration resistor transconductor," in *Proc. 29th Eur. Solid-State Circuits Conf. (ESSCIRC)*, Sep. 2003, pp. 449–452.
[14] J. Lim and J. Kim, "A 20-kHz 16-MHz programmable-bandwidth 4th order active filter using gain-boosted opamp with negative resistance in 65-nm CMOS," *IEEE Trans. Circuits Syst. II, Exp. Briefs*, vol. 66, no. 2, pp. 182–186, Feb. 2019.
[15] J. S. Mincey, C. Briseno-Vidrios, J. Silva-Martinez, and C. T. Rodenbeck, "Low-power $G_m - C$ filter employing current-reuse differential difference amplifiers," *IEEE Trans. Circuits Syst. II, Exp. Briefs*, vol. 64, no. 6, pp. 635–639, Jun. 2017.
[16] M. S. Oliveira, P. C. de Aguirre, L. C. Severo, A. G. Girardi, and A. A. Susin, "A digitally tunable 4th-order Gm-C low-pass filter for multi-standards receivers," in *Proc. 29th Symp. Integr. Circuits Syst. Design (SBCCI)*, Aug. 2016, pp. 1–6.

XIAOYING WANG (Student Member, IEEE) received the B.Eng. degree from Nanyang Technological University (NTU), Singapore, in 2016, where she is currently pursuing the Ph.D. degree in the interdisciplinary graduate program.

Her research interests include analog and RF circuit designs for medical devices, especially analog filter designs for WBAN transceivers.

CHIRN CHYE BOON (Senior Member, IEEE) received the B.E. (Hons.) and Ph.D. degrees in electrical engineering from Nanyang Technological University (NTU), Singapore, in 2000 and 2004, respectively.

He was with Advanced RFIC, Singapore, where he worked as a Senior Engineer. Since 2005, he has been with NTU, where he is currently an Associate Professor. He has been the Program Director for RF and mm-wave research at the $50 Million Research Centre of Excellence, VIRTUS (NTU), since March 2010. He specializes in the areas of radio frequency (RF) and mm-wave circuits design for communications applications. He has conceptualized, designed, and silicon-verified many circuits/chips resulting in over 160 refereed publications and over 30 patents in the fields of RF and mm-wave. He is the coauthor of the book *Design of CMOS RF Integrated Circuits and Systems* and *CMOS Millimeter-Wave Integrated Circuits for Next Generation Wireless Communication Systems* (World Scientific Publishing).

Dr. Boon serves as a committee member for various conferences. He is the Principal Investigator for research grants of over ten million. He is also one of the key NTU-team members of MIT-NTU joint collaboration project "Low Energy Electronic Systems," which has won the Singapore-MIT Alliance for Research and Technology (SMART) International Research Grant (IRG) proposal with a grant total of S$25 million. He is the Program Director for RF and mm-wave research at the $50 Million Research Centre of Excellence, VIRTUS (NTU), since March 2010. He is an Associate Editor for the IEEE TRANSACTIONS ON VERY LARGE SCALE INTEGRATION (VLSI) SYSTEMS. He is the IEEE ELECTRON DEVICES LETTERS Golden Reviewer.

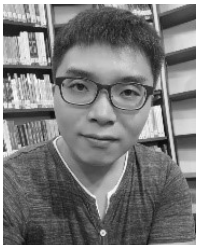

KAITUO YANG (Member, IEEE) received the B.S. and M.S. degrees from the School of Information Science and Technology, University of Science and Technology of China (USTC), in 2011 and 2014, respectively. He is currently pursuing the Ph.D. degree with Nanyang Technological University (NTU), Singapore.

He is also a Researcher with the VIRTUS Laboratory, NTU, since 2014. His research interests include analog and RF integrated circuits and systems for wireless communications, especially focusing on low NF and high linearity receiver design. He holds several patents in the field of RF-CMOS design.

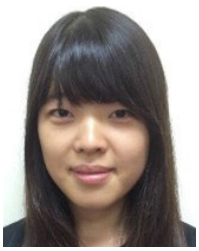

LINGSHAN KONG received the B.Eng. and Ph.D. degrees from Nanyang Technological University (NTU), Singapore, in 2014 and 2019, respectively.

Her research interests include transceiver design for high-speed communication, including wireless receiver design, wireline backplane transceiver design, and wideband analog baseband design.